Journal of Alloys and Compounds 516 (2012) 73–77

Contents lists available at SciVerse ScienceDirect

Journal of Alloys and Compounds

journal homepage: www.elsevier.com/locate/jallcom

The mechanism of enhanced magnetic properties of sintered permanent magnets by substitution of Pr for Nd

Bicheng Chen*, Xingmin Liu, Renjie Chen, Shuai Guo, Don lee, Aru Yan

Division of Magnetic Materials and Advanced Devices, Ningbo Institute of Material Technology and Engineering, Chinese Academy of Sciences, Ningbo, Zhejiang 315201, China

ARTICLE INFO

Article history:
Received 18 October 2011
Received in revised form
24 November 2011
Accepted 26 November 2011
Available online 6 December 2011

Keywords:
Pr–Fe–B
Low Dy
High coercivity
Thermal stability

ABSTRACT

In this study, the influence of substitution of Nd with Pr on the magnetic of sintered permanent magnets was investigated. The samples were prepared by traditional powder metallurgical technique. The nominal composition of the alloys is $(Nd_{1-x}Pr_x)_{29}Dy_{1.3}R_{3.1}Fe_{bal}$ ($R = Al_{0.3}Cu_{0.2}$ $Co_{1.5}$ $B_1Zr_{0.1}$, wt%) with x varying from 0 to 1 in steps of 0.2. Experimental results show that the overall magnetic properties, especially the intrinsic coercivity and thermal stability of the magnets, could be improved by substituting Nd with Pr in the magnets. When the Pr replaces all Nd in the magnets, excellent performance magnets with Br = 13.65 KGs, Hcj = 22.13 KOe, $(BH)_{max}$ = 46.1 MGsOe are obtained with a low Dy content (1.3 wt%).

1. Introduction

The Nd–Fe–B permanent magnet has been widely used in various fields due to the excellent magnetic performance since its discovery [1]. Nd as the principal ingredient of the Nd–Fe–B magnets was consumed greatly. In nature rare earth mine, however, there are many other commensal rare earth elements, such as La, Ce, Pr. These rare earth elements have not been well used in Nd–Fe–B product magnets, especially for Pr. Pr is frequently keeping paragenic with Nd in the ores, and the content of Pr is usually 1/3 of Nd, which is a great reserve volume in nature resources. Besides, Pr is very similar to Nd in both elemental state and in the $RE_2F_{14}B$ compounds; both $Pr_2Fe_{14}B$ and $Nd_2Fe_{14}B$ have a tetragonal structure with a space group $P4_2mnm$, with the same a-spacing of 0.881 nm and closely similar c-spacing of 1.227 and 1.221 nm, respectively [2]. The Curie temperature of $Nd_2Fe_{14}B$ (586 K) is similar to $Pr_2Fe_{14}B$ (569 K), and the saturation magnetization of $Pr_2Fe_{14}B$ (1.56 T) is also comparable to that of $Nd_2Fe_{14}B$(1.60 T) [3]. However, $Nd_2Fe_{14}B$ has a spin reorientation around 140 K [4], leading to a detrimental effect upon the magnetic properties [5] at low temperatures, whereas $Pr_2Fe_{14}B$ exhibits no spin reorientation down to 4.2 K [6] and therefore exhibits superior magnetic properties than those of $Nd_2Fe_{14}B$ at the low temperatures. Furthermore, the anisotropy field of $Pr_2Fe_{14}B$ (8.7 T) is higher than that of $Nd_2Fe_{14}B$ (6.7 T) [7], indicating that a somewhat higher intrinsic coercivity (Hcj) could be obtained in the former. All these factors make Pr–Fe–B magnets attractive for broad temperature range applications, as discussed by Pourarian et al. [8] and Rabinovich et al. [9]. In this study, a systematic research carried out to study the effects of adding Pr in Nd–Fe–B to replace Nd on the magnetic properties, thermal stability of sintered permanent magnets, and the mechanism of the improved magnetic properties was discussed. Experimental results indicate that with the increase of Pr content in the magnets, the microstructure of the magnets was improved, which resulted in the better magnetic properties and thermal stability.

2. Experimental procedures

The powder metallurgy method was adopted in the present work [4,10]. Strip casting technique was employed to prepare the alloys strips with nominal compositions of $(Nd_{1-x}Pr_x)_{29}Dy_{1.3}R_{3.1}Fe_{bal}$ (wt%, $R = Al_{0.3}Cu_{0.2}$ $Co_{1.5}$ $B_1Zr_{0.1}$) with x varying from 0 to 1 in steps of 0.2. The strips were crushed by hydrogen decrepitating (HD) treatment, and then jet milled (JM) under N_2 gas flow. The powder was pressed and simultaneously aligned in a magnetic field of 2 T, and then isostatic pressed under a pressure of 300 MPa for 60 s. The green compacts were sintered at a series temperature from 1050 °C to 1075 °C for 2.5 h to obtain the full density magnets, then annealed at 900 °C for 1.5 h and at 500 °C for 2 h. All these heat treatments were under a vacuum around 4.5×10^{-4} Pa and cooled at room temperature under positive pressure of Ar gas. The particle size of the powder was analyzed by Laser Particle Size Analyzer (HELOS/BF-OM). All samples were cut into column in size of φ 10 mm × 10 mm by wire-electrode cutting. The magnetic properties were measured by NIM-500C hysteresigraph. Curie temperature of the

---

* Corresponding author.
E-mail address: cbc98cbc@163.com (B. Chen).

0925-8388/$ – see front matter © 2011 Elsevier B.V. All rights reserved.
doi:10.1016/j.jallcom.2011.11.132

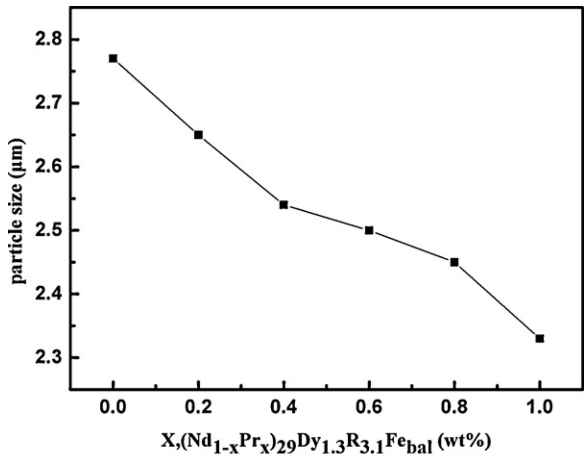

Fig. 1. The average particle size for the $(Nd_{1-x}Pr_x)_{29}Dy_{1.3}R_{3.1}Fe_{bal}$ (wt%, $x = 0$, 0.2, 0.4, 0.6, 0.8, 1) powders.

magnets was measured by DSC NETZSCH-404C. The microstructure investigation was carried out by SEM (TM-1000 and S4800) and TEM (Tenai F20). X-ray diffraction was done on the magnet using Cu_α K radiation on a Bruker AXS D8 advance diffractometer.

3. Results and discussion

3.1. The particle size of JM powders

A comparison of the particle size for the six composition $(Nd_{1-x}Pr_x)_{29}Dy_{1.3}R_{3.1}Fe_{bal}$ (wt%, $x = 0$, 0.2, 0.4, 0.6, 0.8, 1, $R = Al_{0.3}Cu_{0.2}$ $Co_{1.5}$ $B_1Zr_{0.1}$) powders which were jet milled under the same condition is shown in Fig. 1. The average particle size decreases from 2.77 μm to 2.33 μm as the Pr addition content increases from 0 to 100 wt%. This is because the toughness of the strip casting ribbons becomes lower with the decreases of Nd content [11,12]. In the jet milling process, the ribbons with higher Pr content are easily crushed into fine particle size powder, which means that fine JM powders could be obtained by increasing the Pr content in the alloys. In this study, in order to avoid the influence of the particle size on the magnetic properties, we tried the different jet mill parameters to obtain JM powders with the similar average particle size. Since Sagawa [13] reported that the smaller particle size is in favor of high performance of the magnets, we control the JM process to make the average particle size of the powders for the six alloys around 2.45 μm, which is smaller than traditional particle size 3–5 μm adopted in NdFeB production [14], to optimize the magnetic properties.

3.2. Magnetic properties

Fig. 2(A) and (B) shows a comparison of demagnetization curves and magnetic properties of the samples with different Pr contents. One can see that the Hcj increases from 14 KOe to 22 KOe with the increasing of Pr content. Both Br and BHm seem to be less sensitive to the Pr content, and the values are similar without regularity, which is probably due to the saturation magnetization of $Pr_2Fe_{14}B$ comparable to that of $Nd_2Fe_{14}B$ (1.56 T compared with 1.60 T) [3] and the density of the magnets are similar. However, the Br of the magnet is increased from 13.5 KGs ($x = 0.2$) to 13.83 KGs ($x = 0.6$), which could be attributed to the different grain alignment of the magnets. It was reported that an increase in the degree of grains alignment of sintered magnets is in favor of high Br [15]. Fig. 3 shows the XRD pattern of the magnets, the grain alignment is described by the ration of I_{006} to I_{105}, the higher value of I_{006}/I_{105}, the better grain alignment of the magnet. It can be seen from Fig. 3 that the value of I_{006}/I_{105} increases from 0.948 ($x = 0.2$) to 1.134 ($x = 0.6$), which corresponds with the Br increased from 13.5 KGs ($x = 0.2$) to 13.83 KGs ($x = 0.6$). Although I_{006}/I_{105} reaches the max value when $x = 1$, the Br is not as high as the former, which could be due to the low saturation magnetization of Pr-based magnets. Whether the grain alignment is related to the Pr content in the magnet needs the further study.

There are three reasons responsible for the increase of Hcj as the Pr content increases in the magnets. Firstly, Hcj is related to the ansistropy field H_A of the main phase ($RE_2Fe_{14}B$) in the magnets. The ansistropy field H_A of $Pr_2Fe_{14}B$ is 6920 KA m^{-1}, which is higher than that of $Nd_2Fe_{14}B$ (5530 KA m^{-1}). As the Pr content increases in the magnets, H_A enhanced as more $Pr_2Fe_{14}B$ phase formed, and thus higher Hcj. Secondly, Hcj is closely related to the grain size of the magnets, the small grains are in favor of high Hcj [16]. SEM investigation of the samples found that the grains for Nd-based magnets are bigger than that of Pr-based magnets and the grains size tends to become smaller as the Pr content increases in the magnets. Fig. 4(A) and (B) shows the microstructure of the magnets with substitution of Nd with Pr for 0 and 100 wt% respectively. The black regions are the grain boundary phases (RE-rich phase) being etch off by chemical corrosion during samples preparation. It can be seen that the overall appearance of the grains is bigger in Fig. 4(A) compared with those seen in Fig. 4(B), most grains of Nd-based magnets are larger than that of Pr-based magnets. As the grains become smaller, Hcj is improved. The different grains size of the magnets

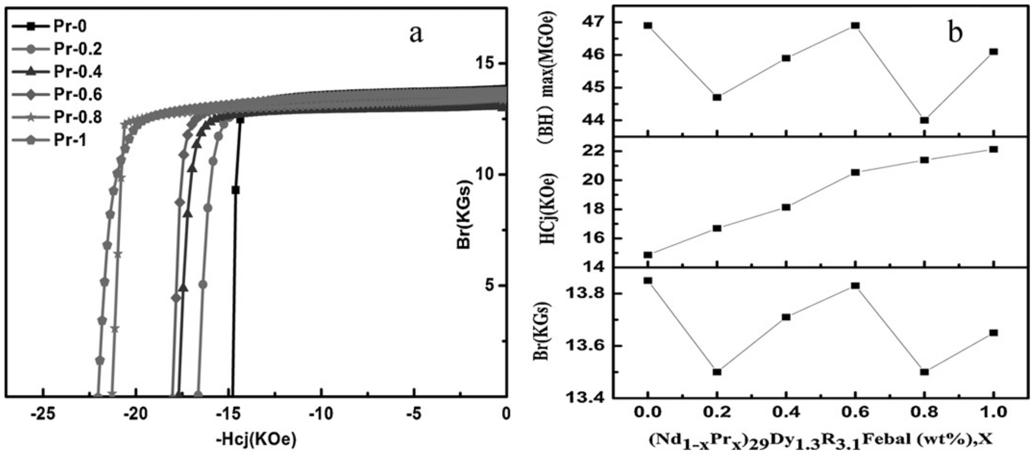

Fig. 2. Demagnetization curves (A) and magnetic properties (B) for magnets $(Nd_{1-x}Pr_x)_{29}Dy_{1.3}R_{3.1}Fe_{bal}$ (wt%, $x = 0$, 0.2, 0.4, 0.6, 0.8, 1).

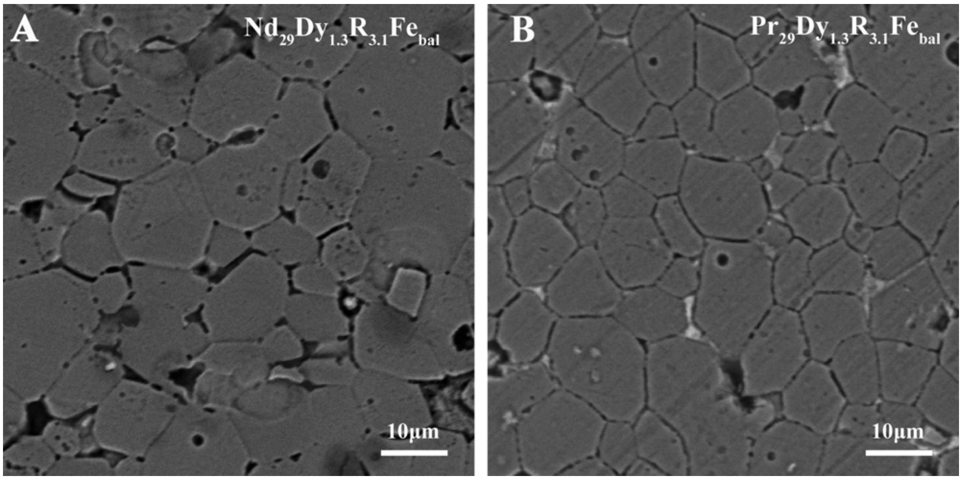

Fig. 3. XRD patterns for $(Nd_{1-x}Pr_x)_{29}Dy_{1.3}R_{3.1}Fe_{bal}$ (wt%, $x = 0, 0.2, 0.4, 0.6, 0.8, 1$).

could be due to the different sintering behaviors of Pr-based and Nd-based magnets. The Pr-based magnets can be sintered to saturation density at a relatively lower sintering temperature than that of Nd-based magnets [17], and the lower sintering temperature is in favor of obtaining the smaller grains size. Besides, Nd-based magnets exhibit more grain growth than the corresponding Pr-based magnets [2], which indicate that adding Pr in the magnets to replace Nd can reduce the grains size and thus improve Hcj of the magnets.

Thirdly, the grain boundary (GB) phase plays an important role in determining the Hcj. It was found in our study that Pr additions can smooth the GB and optimize the GB phase. Fig. 5 shows the back-scattered electron micrographs and HRTEM images of the Pr-free and Pr-based magnets, Fig. 5(A) and (B) shows back-scattered electron micrographs, the black regions are the main phase ($RE_2Fe_{14}B$), and the white regions which surround the main phase are the RE-rich phase. Fig. 5(C) and (D) shows the detail GB information for Pr-free and Pr-based magnets. It can be seen from Fig. 5 that the GB of Pr-free magnets is irregular and not smooth. There exist serrated edges in the GB. This kind of GB can generate the local demagnetization field on the grain surface and to form magnetically reverse domains [16] and thus worsen the Hcj of the magnets. While for the Pr-based magnets, the surface defects of the grains are decreased, which reduce the possibility of nucleation of reversal walls that may deteriorate Hcj of the magnets. The different GB shape could be due to $Pr_2Fe_{14}B$ being more soluble in Pr-rich liquid phase during sintering process [2], which will make small $Pr_2Fe_{14}B$ particles and sharp edges of the grains dissolute in the Pr-rich liquid phase during Solution RE-precipitation stage of the liquid phase sinter process [16], and thus smooth the GB. Some discontinuous grain boundaries phase (RE-rich phase) can be seen for Pr-free magnets, while for the Pr-based magnets, the grain boundaries phase are clear and continuous. This is probably because that the Pr doping improves the soakage property of liquid phases and lubricates the grain boundary to form the smooth RE-rich intergranular phase, resulting in effectively separating the magnetic grains, weakening the exchange couple demagnetization effect and improving the Hcj of magnets.

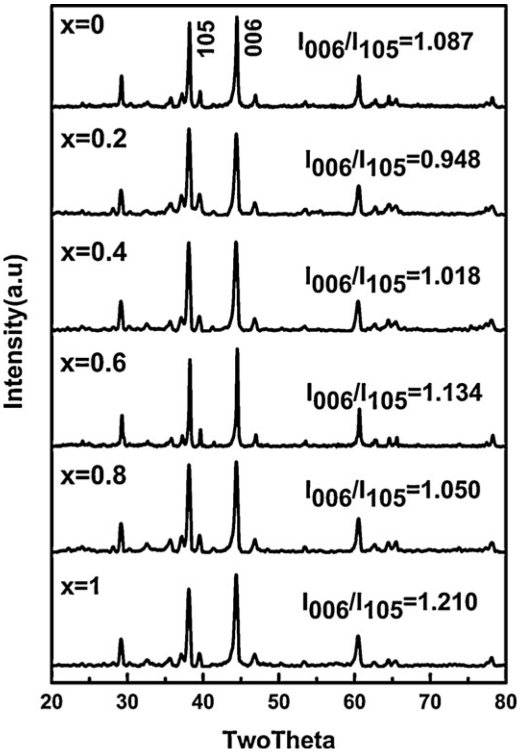

Fig. 4. SEM image for Nd-based and Pr-based magnets.

3.3. *Curie temperature and thermal stability*

The thermal stability is a very important parameter for the application of sintered permanent magnets at high working temperature. Table 1 shows the magnetic properties at temperature of 20 °C and 100 °C respectively, and the Curie temperature (Tc) of the magnets is also shown in Table 1. The Br and Hcj temperature coefficients α and β were calculated by Eqs. (1) and (2) respectively.

$$\alpha\ (\%) = \frac{\mathrm{Br}(T) - \mathrm{Br}(T_0)}{\mathrm{Br}(T_0)(T - T_0)} \times 100 \tag{1}$$

$$\beta(\%) = \frac{\mathrm{Hcj}(T) - \mathrm{Hcj}(T_0)}{\mathrm{Hcj}(T_0)(T - T_0)} \times 100 \tag{2}$$

It can be found that α does not change after adding the Pr, while β is improved as the Pr content increased, which could be due to the improved Hcj at room temperature. It was reported that the absolute value of β decreased with increasing Hcj and the ratio of microstructure parameter c (varies with the grain size) to N_{eff} (varies with the smoothness of the grain boundaries) for sintered $RE_2Fe_{14}B$ magnet, indicating that the increase of Hcj and c/N_{eff} can effectively decrease the value of β [18]. In this study,

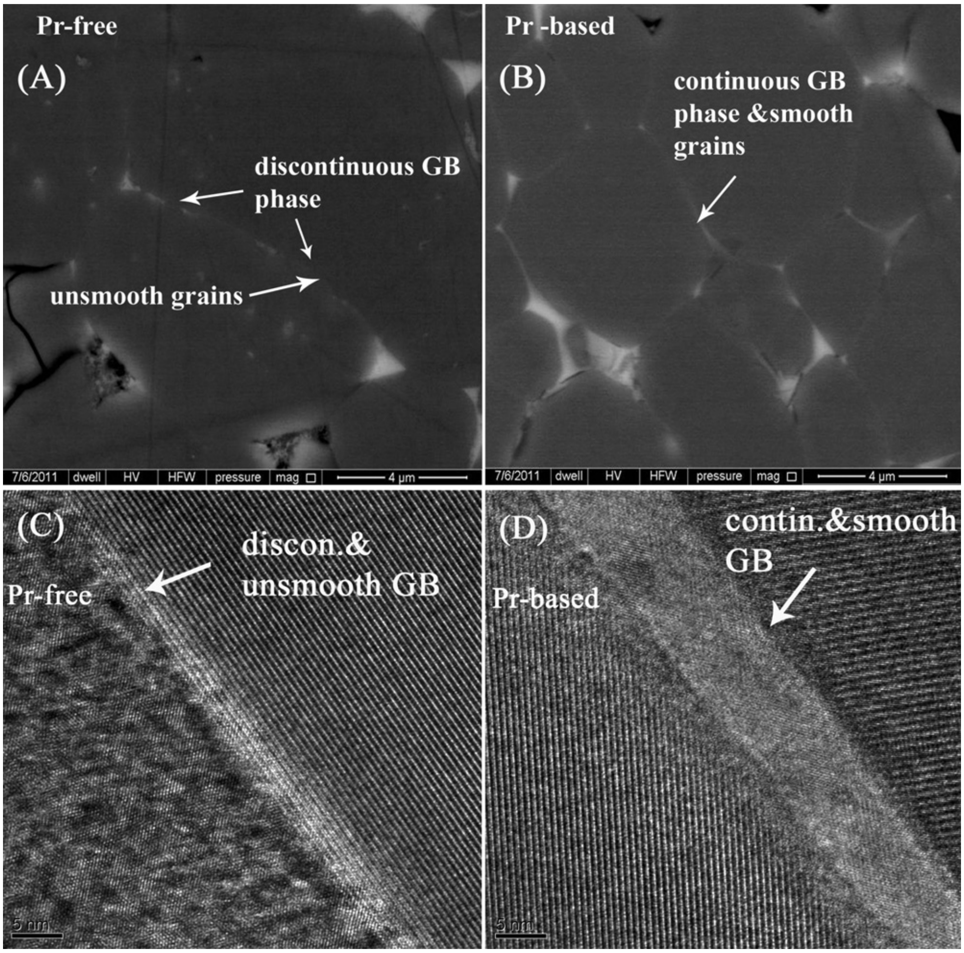

Fig. 5. Back-scattered electron micrographs and HRTEM images for Pr-free and Pr-based magnets.

Table 1
Magnetic properties and thermal stability of $(Nd_{1-x}Pr_x)_{29}Dy_{1.3}R_{3.1}Fe_{bal}$ (wt%, $x = 0, 0.2, 0.4, 0.6, 0.8, 1$).

$(Nd_{1-x}Pr_x)_{29}Dy_{1.3}R_{3.1}Fe_{bal}$ (x)	Br (KGs)	Hcj (KOe)	$(BH)_{max}$ (MGsOe)	Temp. (°C)	A (%/°C)	β (%/°C)	Tc (°C)
0	14.07	14.86	48.3	20			325
	12.93	6.18	39.79	100	0.101	0.73	
0.2	13.5	16.69	44.7	20			322
	12.42	7.17	36.56	100	0.10	0.713	
0.4	13.71	18.14	45.9	20			320
	12.5	7.97	37.06	100	0.11	0.70	
0.6	13.83	20.54	46.9	20			317
	12.55	9.09	37.37	100	0.115	0.697	
0.8	13.5	21.39	44	20			315
	12.3	9.57	35.61	100	0.111	0.69	
1	13.65	22.13	46.1	20			312
	12.45	10.04	36.64	100	0.109	0.682	

as the Pr substitute Nd in the magnets, Hcj was improved, grains of the magnet were refined (shown in Fig. 4), grain boundaries were improved (shown in Fig. 5). All these factors make the value of β improved. The result is also concordant with Cui et al. [18] report. Previous studies have shown that β could be improved by substitution of heavy rare-earth Dy for Nd [19], but the saturation magnetic polarization of $Dy_2Fe_{14}B$ (0.7 T) is much lower than Nd2Fe14B (1.6 T) and Pr2Fe14B (1.56 T) [3], low saturation polarization decrease both Br and $(BH)_{max}$, and also Dy is much expensive. Our experiment results reveal that the temperature stability of the magnet could be improved by adding Pr, while avoiding the deterioration of Br and $(BH)_{max}$. The Tc of the magnets decreases very slightly as the Pr content increases because the Tc of compounds $Nd_2Fe_{14}B$ (586 K) and $Pr_2Fe_{14}B$ (569 K) [3] is very close.

4. Conclusions

Substitution of Nd by Pr in the magnets can lead to the improvement of the soakage property of liquid phases and make a lower temperature sintering possible, thus restrain the abnormal grain growth and in favor of obtaining magnets with the grain size of $RE_2Fe_{14}B$ phase refined, and the grain boundaries also become clear and smooth, RE-rich phase surrounds the main phase more continuous. All these factors result in the improvement of Hcj and thermal stability of the magnets. By adding Pr to replace Nd in the Nd–Fe–B magnets, we successfully prepared low Dy(1.3 wt%) sintered magnets with excellent magnetic properties of Br = 13.65 KGs, Hcj = 22.13 KOe, $(BH)_{max}$ = 46.1 MGOe. There is little influence of Tc as the Pr substitution.

Acknowledgments

This work was supported by National Basic Research Program (No. 2010CB934601) of China and Major Scientific and Technological Special of Zhejiang (No. 2007C11046).

References

[1] M. Sagawa, S. Fujimura, N. Togawa, H. Yamamoto, Y. Matuura, J. Appl. Phys. 55 (1984) 2083.
[2] M.R. Corfield, A.J. Williams, I.R. Harris, J. Alloys Compd. 296 (2000) 138.
[3] E.P. Wohlfarth, K.H.J. Buschow (Eds.), Ferromagnetic Materials, vol. 4, North-Holland, Amsterdam, 1988, p. 20.
[4] J.J. Croat, J.F. Herbst, R.W. Lee, F.E. Pinkerton, J. Appl. Phys. 55 (1984) 2078.
[5] S. Heisz, HilscherF G., J. Magn. Magn. Master. 67 (1987) 20.
[6] E.B. Boltich, W.E. Wallace, Solid State Commun. 55 (1985) 529.
[7] S. Hirosawa, Y. Matsuura, H. Yamamoto, S. Fujimura, M. Sagawam, H. Yamauchi, J. Appl. Phys. 59 (1986) 873.
[8] F. Pourarian, S. Simizu, R.T. Obermyer, S.G. Sankar, W.E. Wallace, 11th International Workshop on Rare-earth Magnets and their Application, Pittsburgh, 1990, p. 401.
[9] Y.M. Rabinovich, S. Szymura, J.J. Wyslocki, H. Bala, J. Magn. Magn. Mater 140–144 (1995) 1065–1066.
[10] A.H. Li, S.Z. Dong, W. Li, Sci. China G 46 (2003) 241.
[11] S. Liu, D. Cao, R. Leese, Proceedings of 17th Workshop on REPM, Delaware, Newark, USA, 2002, p. 360.
[12] J.F. Liu, P. Vora, M.H. Walmer, E. Kottcamp, J. Appl. Phys. 97 (2005) 10H101–11H.
[13] M. Sagawa, The Nd–Fe–B magnet from birth to 100,000 ton/year giant, IEEE International Magnetics Conference, Taipei, 2011.
[14] S.-G. Zhang, H. Li, J. Zhao, et al., J. Rare Earths 6 (2002) 589.
[15] R.N. Faria, A.R.M. Castro, N.B. Lima, J. Magn. Magn. Mater. 238 (2002) 46.
[16] S.Z. Zhou, Q.F. Dong, Super Permanent Magnets – Permanent Magnetic Material of Rare-earth and Iron System, Metallurgy Industry Publishing, Beijing, 2004.
[17] M.G. Taylor, B.E. Davies, I.R. Harris, J. Magn. Mater. 242-245 (2002) 1375.
[18] X.G. Cui, M. Yan, T.Y. Ma, W. Luo, S.J. Tu, Sci. Sinter. 41 (2009) 91.
[19] G. Bai, R.W. Gao, Y. Sun, G.B. Han, B. Wang, J. Magn. Magn. Mater. 308 (2007) 20.